Nuclear Magnetic Resonance Measurements in Solid He^3†

M. G. RICHARDS,* J. HATTON, AND R. P. GIFFARD
The Clarendon Laboratory, Oxford, England
(Received 8 February 1965)

Measurements of the magnetic susceptibility of solid He^3 are complicated by the nature of the coupling of the spin system to the lattice. This coupling is examined at temperatures down to 0.1°K, magnetic fields up to about 2 kG, and molar volumes between 18.5 and 24 cm^3 using a continuous-wave nmr apparatus. For pure He^3, the three-bath model of Garwin and Landesman gives a good description of the way in which the spins achieve equilibrium with the lattice. By measuring the various relaxation times, values of the exchange integral are derived by several different methods with good internal consistency. Values of the exchange-bath specific heat very close to the calculated values are observed. We have measured values of the exchange-lattice relaxation time over the same wide range of temperature and molar volume and find values very different from the results of Garwin and Reich. This and their large discrepancy between observed and calculated exchange-bath specific heats we believe to be due to the presence of about 1% He^4 in their samples. In the bcc phase, over certain temperature regions, diffusion appears to be the dominant coupling process, and values of the self-diffusion coefficient are calculated which suggest that the diffusion process is thermally activated at values down to at least 10^{-16} cm^2 sec^{-1}. Experiments on samples containing 0.5% He^4 show that the presence of small amounts of He^4 impurity affects very strongly certain parameters in the three-bath model, and concentrations as low as 0.05% are detectable by their effect on the exchange-bath specific heat. Also in the impure samples a new long relaxation time appears below 0.7°K, which we believe was incorrectly identified as the exchange-lattice relaxation time by Garwin and Reich and which was the cause of nonequilibrium between spins and lattice in the magnetic susceptibility experiments of Adams, Meyer, and Fairbank.

I. INTRODUCTION

THE properties of solid He^3 at very low temperatures depend to a large extent on the exchange interaction between the atoms. This interaction can be measured by means of nuclear magnetic resonance experiments, and it is now possible to give reliable quantitative results for the exchange interaction in solid He^3 at different molar volumes.

Nuclear-magnetic-resonance studies in solid He^3 are of special interest also on account of the way in which thermal equilibrium between the nuclear spins and the lattice is attained. At temperatures below 1°K, the Zeeman energy of the nuclear-spin system relaxes to the lattice according to the model (which we shall call the three-bath model) first proposed for He^3 by Garwin and Landesman,[1] via an intermediate reservoir which represents the exchange energy of the crystal. Using this model to analyze the recovery of the Zeeman temperature following saturation in large resonant radiofrequency fields, we have obtained values for the heat capacity of the exchange system and for the relaxation times between the Zeeman, exchange, and lattice reservoirs. Results have been obtained for He^3 at molar volumes in the range from 18.5 to 24.0 cm^3, at temperatures down to 0.1°K using resonance frequencies between 1 and 5 Mc/sec, and represent an extension of preliminary results reported earlier.[2]

Some of the parameters occurring in the three-bath model appear to be strongly influenced by the presence of small quantities of He^4. Measurements made on He^3 containing different amounts of He^4 lead us to believe that the properties of pure He^3 will not be essentially different from those of our purer samples and enable us to resolve some serious inconsistencies which were present in published work of other investigators.[1,3]

II. EXPERIMENTAL

A. Sample Cell

The sample cell, shown with part of the cryostat in Fig. 1, is a hollow, thick-walled cylinder of German silver holding about 0.3 cm^3 of He^3. The He^3 is fed in through a capillary tube B which, between the sample cell and the 1°K liquid He^4 bath, consists of 25 cm of cupronickel tube of i.d. 0.3 mm and o.d. 1.5 mm wound in the form of a helix. The sample cavity is lined with a piece of crystalline fluorite C to act as a nuclear magnetic resonance thermometer, and inside this liner is situated the rf coil. A carbon resistor D is cemented into the outside wall of the German silver pot to serve as a secondary thermometer.

In order to form He^3 samples of known molar volume we use the fact that, while maintaining the fluid phase

† Some of the research reported in this paper was made possible through the support and sponsorship of the U. S. Army through its European Research Office.
* Present address: University of Sussex, Brighton, United Kingdom.
[1] R. L. Garwin and A. Landesman, in *Proceedings of the Eighth International Conference on Low-Temperature Physics, London, 1962* (Butterworths Scientific Publications Ltd., London, 1963), p. 56; R. L. Garwin and A. Landesman, Phys. Rev. **133**, A1503 (1964).
[2] B. T. Beal, R. P. Giffard, J. Hatton, M. G. Richards and P. M. Richards, Phys. Rev. Letters **12**, 393 (1964). Referred to in this work as PRL. M. G. Richards, J. Hatton and R. P. Giffard, Proceedings of the Ninth International Conference on Low Temperature Physics, Columbus, Ohio, 1964 (to be published).
[3] R. L. Garwin and H. A. Reich, Phys. Rev. Letters **12**, 354 (1964).

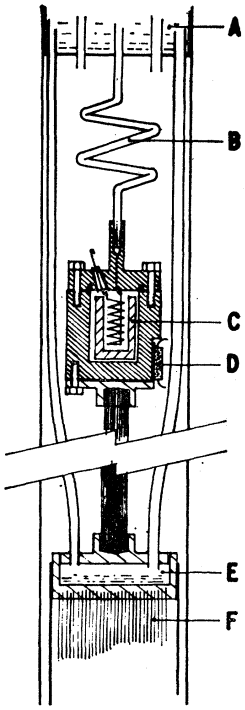

FIG. 1. Sample chamber and part of cryostat. A, 1°K liquid helium bath. B, capillary filling line. C, fluorite liner. D, carbon resistance thermometer. E, He^3 cryostat. F, chrome alum salt pill with copper-foil vanes.

in the sample cell, the capillary can be blocked with solid in the region where it passes through the liquid He^4 bath simply by reducing the temperature of this bath. From published[4] data of the *PVT* values on the melting line of He^3, we then know the molar volume at which the sample has been sealed off in the cell.

The nuclear spin-lattice relaxation times of the solid and fluid phases on the melting line are very different, so that by observing the nmr signal in an rf resonant field sufficiently strong to produce saturation, it is possible to detect about 1% of solid in the liquid or 5% of the liquid in the solid. This provides a useful check on the molar volume through the temperature of the onset and completion of the solidification process at constant volume.

Samples of molar volume 24 cm^3 and greater are difficult to form in our apparatus because the capillary must then be cooled to about 1°K to block it. Any He^3 entering the sample chamber during solidification can be detected by observing the pressure in the room-temperature part of the system. The volume at room temperature is small, so that an increase of 1% in the molar volume of the sample would be revealed in this way.

B. Fluorite Thermometer

The magnetic susceptibility of the F^{19} nuclei in fluorite can be expected to obey Curie's law down to temperatures in the microdegree region, since the internal magnetic field arises primarily from nuclear dipole moments in a rigid lattice. From an experimental point of view, the F^{19} resonance is convenient to use for thermometry in our investigations because it can be measured with the same equipment as is used for the He^3 resonance experiments. It is, of course, essential that the spin-lattice relaxation time of the F^{19} nuclei be sufficiently short—a requirement which has been met by choosing fluorite containing an appropriate amount of electron-paramagnetic impurities.

When the fluorite susceptibility is to be measured, the frequency of the rf field is switched to the new resonance value which is 25% higher and the resonant frequency of the tuned circuit adjusted. We then sweep slowly through the line while applying a field modulation of 1 G and measure the signal by means of a lock-in amplifier. The signal and therefore the temperature can be measured to about 1% in the range 1.0 to 0.5°K, where the vapor pressure of He^3 can be used for calibration purposes.

C. Electronics

A continuous-wave apparatus using the Rollin[5] method of detection is employed. The range of frequency is approximately 1–5 Mc/sec, the lower limit being due to low signal-to-noise ratio and the upper one being determined by the capacity of the input circuit. In the middle frequency region, the Q of the input circuit is about 15.

In most of the measurements, the dc magnetic field is modulated at some audio frequency between 15 and 50 cps with an amplitude many times the resonant linewidth, and the signal is displayed on an oscilloscope. For susceptibility measurements this signal can also be fed into an amplifier tuned to twice the modulation frequency, giving rise to an output proportional to the

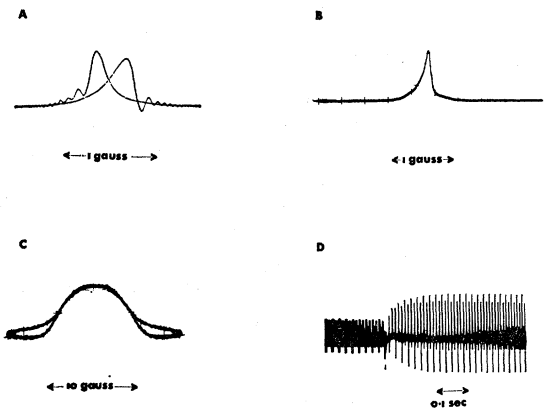

FIG. 2. Oscillograms showing the He^3 signal with af modulation (A) and single slow sweep (B). C shows the F^{19} signal with af modulation and D shows a recovery of the He^3 signal following an increase in the af modulation amplitude, using a linear time base for display.

[4] E. R. Grilly and R. L. Mills, Ann. Phys. (N. Y.) 8, 1 (1959).

[5] J. Hatton and B. V. Rollin, Proc. Roy. Soc. (London) **A199**, 222 (1949).

area of the absorption signal. It is also possible, using dc coupling from the detector to the oscilloscope, to display signals produced by a single slow passage through resonance. Typical oscillograms are shown in Figs. 2(a) and 2(b), the former with af modulation and the latter due to a single sweep through resonance. The width of the He^3 resonance which is about 0.1 G is due to external field inhomogeneity. Figure 2(c) shows the F^{19} resonance with af modulation.

The conventional procedure for measuring the spin-lattice relaxation time τ_1 with this type of apparatus, namely by observing the rate of signal recovery after saturating with rf power, becomes difficult when τ_1 is much less than a few seconds. There are problems connected with recording the signal and also with the recovery time of the amplifier following large changes in carrier voltage. These difficulties have been avoided by a method which enables values of τ_1 down to about 10 msec to be measured. The method depends on changing the rf power fed into the nuclear spin system by changing the amplitude of the field modulation. With the dc field set accurately to its resonant value, a modulation through about 20 G at audio-frequency f_{mod} is applied. To saturate, the width of modulation is reduced temporarily to about 0.2 G so that the mean rf power fed into the spin system is correspondingly increased. On returning the field modulation to the high value, the rf power input is reduced and the signal recovers from the saturation. To measure the recovery, the signal is displayed on an oscilloscope using a linear time base whose repetition frequency is between 10 and 100 times less than f_{mod}. The oscillogram, a typical example of which is shown in Fig. 2(d), therefore consists of a series of peaks separated by a time $(2f_{\text{mod}})^{-1}$, each of which gives a measure of the nuclear polarization at that instant. With $f_{\text{mod}}=50$ cps, it is possible in this way to measure values of τ_1 as short as 10 msec with fair accuracy. In cases where it is desired to saturate the spin system for only a very short time, the field modulation may be reduced for just one passage through resonance by a relay and pulse generator.

III. RESULTS IN PURE He^3

A. He^3 Purity

The first experiments in this investigation were made on He^3 containing 0.5% He^4. The results were characterized by large discrepancies between values for the heat capacity of the exchange bath obtained by different methods, as will be discussed in more detail later. In an attempt to discover the origin of these discrepancies, the He^3 was purified by distillation. It was found that the discrepancy was very much smaller for He^3 containing 0.09% He^4 and had become undetectable (at least in the bcc phase) when the He^4 content had been reduced to 0.05%. For this reason we shall describe measurements on He^3 containing not more than 0.05% He^4 as relating to pure He^3. It will appear later however that this supposition may not be justified for the hcp phase.

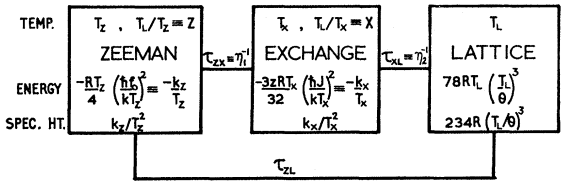

FIG. 3. The three-bath model.

B. The Three-Bath Model

We suppose that the contributions to the total energy of solid He^3 in a magnetic field which are important for our purpose are (i) the Zeeman energy, (ii) the exchange energy, and (iii) the lattice energy. It was shown by Garwin and Landesman[1] that these three baths may be characterized by different temperatures provided that the exchange frequency is greater than the frequency with which atoms change their position in the lattice due to diffusive jumps.

Figure 3 gives a diagram of the three-bath model with the energy and specific heat of each bath given. The expressions for the first two baths are calculated in Sec. IIIE and the lattice energy is given using a Debye model.

At high temperatures the diffusive motion of the atoms provides the dominant relaxation mechanism. As the temperature is lowered, the average frequency of jumps for each atom τ_c^{-1} is reduced until eventually the local dipole field is modulated more effectively by the exchange interaction. Assuming that the exchange bath is well coupled to the lattice, the spin energy now passes via the exchange bath to the lattice. As the temperature is further lowered, an increasing relaxation time suggests that the exchange-lattice coupling becomes the bottleneck for transfer since the Zeeman-exchange coupling is temperature-independent.

Figure 4 plots the observed recovery time for He^3 of molar volume 20 cm^3 at a resonance frequency, $\omega_0/2\pi$, of 4.8 Mc/sec. Four regions are distinguished. In the first, labelled 0, the relaxation is proceeding from spins direct to lattice. The minimum, which occurs when $\omega_0\tau_c\approx 1$, is a typical feature of relaxation of the Bloembergen-Purcell-Pound (BPP) type. In the temperature-independent region I, the relaxation route is via the exchange bath with the Zeeman-exchange coupling being the bottleneck for energy transfer. In region III the exchange-lattice coupling has become the bottleneck. Region II is an intermediate region where the recovery rate is determined by both τ_{ZX} and τ_{XL} and nonexponential recoveries can, in principle, be observed.

We may regard as unimportant the general case of the spin energy relaxing both directly to the lattice and via

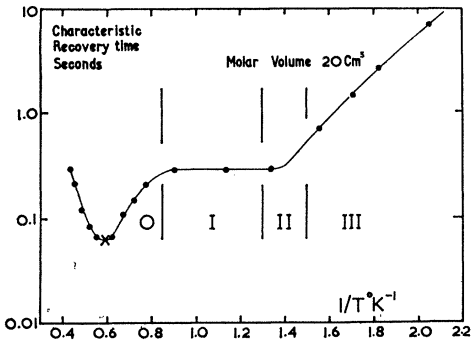

FIG. 4. The temperature variation of the observed characteristic recovery time of the spin system in solid He^3 at a molar volume of 20 cm^3 and a resonance frequency of 4.8 Mc/sec. Regions O-III are explained in the text.

the exchange bath because τ_{ZL} varies as $e^{\theta/T}$ (where θ is the activation temperature for diffusion) and in a very small temperature range we shall pass from $\tau_{ZL}\ll\tau_{ZX}$ to the reverse inequality holding. We should, however, point out that the spins do not relax according to $\tau_Z^{-1}=\tau_{ZX}^{-1}+\tau_{ZL}^{-1}$ because, as discussed by Hartmann,[6] the modulation of the dipole field by diffusive motion and by exchange are not independent. As a result we should say that above a temperature T^* defined by the small transition region discussed above, we cannot characterize the exchange bath by a temperature and we have only two baths. Below T^* we have three baths in series because the direct Zeeman-lattice route can be ignored.

C. The Zeeman-Exchange Relaxation Time

The mechanism by which the exchange interaction modulates the local dipole field and thereby couples the Zeeman and exchange baths has been discussed in detail by Hartmann.[6] We give here a simple derivation which is similar to that used by Garwin and Landesman[1] but gives a different result for one of the key parameters.

We start by assuming the BPP formula for spin relaxation[7]:

$$1/\tau_1=(\tfrac{3}{2})\gamma^4\hbar^2I(I+1)[J_1(\omega_0)+J_2(2\omega_0)], \qquad (1)$$

where

$$J_i(\omega)=\int_{-\infty}^{\infty}G_i(\tau)e^{-i\omega\tau}d\tau,$$

$$G_i(\tau)=\langle F_i(t)F_i(t+\tau)\rangle_{\rm av},$$

$$F_1(t)=\sum_{j>k}[r_{jk}(t)]^{-3}\sin\theta_{jk}(t)\cos\theta_{jk}(t)\exp[-i\phi_{jk}(t)],$$

$$F_2(t)=\sum_{j>k}[r_{jk}(t)]^{-3}\sin^2\theta_{jk}(t)\exp[-2i\phi_{jk}(t)];$$

where $r_{jk}(t)$, $\theta_{jk}(t)$, $\phi_{jk}(t)$ are the spherical polar coordinates of the jth spin referred to the kth spin.

For convenience we shall write

$$G_i(\tau)=k_i(0)g_i(\tau),$$

where $g_i(\tau)$ is a reduced correlation time which is 1 when $\tau=0$ and $\to 0$ as $\tau\to\infty$.

We shall assume, as is usual,

$$g_1(\tau)=g_2(\tau),$$

and

$$k_2(0)=4k_1(0),$$

giving

$$1/\tau_1=(\tfrac{3}{2})(\gamma H_{\rm loc})^2\int_{-\infty}^{+\infty}g(\tau)(e^{-i\omega_0\tau}+4e^{-2i\omega_0\tau})d\tau, \qquad (2)$$

where

$$(\gamma H_{\rm loc})^2\equiv\gamma^4\hbar^2I(I+1)k_1(0). \qquad (3)$$

Before proceeding, we now have to obtain expressions for $g(\tau)$. We consider the two cases which apply to regions O and I of Fig. 4.

Case (i): Diffusion Modulation

We either assume $g(\tau)=e^{-\tau/\tau_c}$ (BPP approach) or follow Torrey[8] who considered the effect of diffusive jumps in more detail and obtained a tabulated function for J_i. Since we are only concerned with the position of the minimum in τ_{ZL} we may summarize the results of these two theories as giving,

$$1/(\tau_{ZL})_{\rm min}=4.3(\gamma H_{\rm loc})^2/\omega_0\ ({\rm BPP}), \qquad (4)$$

$$1/(\tau_{ZL})_{\rm min}=3.9(\gamma H_{\rm loc})^2/\omega_0\ ({\rm Torrey}). \qquad (5)$$

Torrey also gives

$$k_1(0)=(2/15)\sum_k r_k^{-6}, \qquad (6)$$

where r_k is the distance from one spin to the kth spin.

Case (ii): Exchange Modulation

It is usual to write $g(\tau)=\exp(-\frac{1}{2}\omega_e^2\tau^2)$, where ω_e is a frequency of the order of J. Some justification for this comes from the fact that in the expansion of $g(\tau)$ in powers of τ it can be shown that the term in τ is zero. Hartmann[6] calculates the coefficient of τ^2 to obtain an expression for ω_e. Equation (2) now gives

$$1/\tau_{ZX}=[3(2\pi)^{1/2}(\gamma H_{\rm loc})^2/2\omega_e]\times[\exp(-\omega_0^2/2\omega_e^2)+4\exp(-2\omega_0^2/\omega_e^2)]. \qquad (7)$$

We now follow Garwin and Landesman's procedure of relating $(\tau_{ZX})_{\omega_0\to 0}$ to τ_2 and hence to J the exchange in-

[6] S. R. Hartmann, Phys. Rev. **133**, A17 (1964).
[7] A. Abragam, *The Principles of Nuclear Magnetism* (Oxford University Press, New York, 1961), p. 291.
[8] H. C. Torrey, Phys. Rev. **92**, 963 (1953); **96**, 690 (1954).

teraction. This gives for the bcc phase,

$$\left[\frac{1}{\tau_{ZX}}\right]_{\omega_0\to 0}=\frac{15(2\pi)^{1/2}(\gamma H_{\rm loc})^2}{2\omega_e}=\frac{10}{3(\tau_2)_\infty}$$

$$=\frac{10}{3}\left[\frac{1.1\times 10^{11}}{JV^2}\right]; \quad (8)$$

$(\tau_2)_\infty$ is the transverse relaxation time that would be measured at fields such that $\gamma H_0 \gg J$. The last equality, which comes from a detailed examination of the way the exchange "motion" narrows the resonance line, is taken from Garwin and Landesman's paper.

Equation (8) gives us the required relation between ω_e and J provided we have a value for $(\gamma H_{\rm loc})^2$. For this we can use Eqs. (4) or (5) together with an observed value for $(\tau_{ZL})_{\rm min}$. Alternatively we may use our definition of $(\gamma H_{\rm loc})^2$ [Eq. (3)] and Torrey's value for $k_1(0)$. For a bcc lattice, Torrey gives

$$k_1(0)=(58/15)(\sqrt{3}/2l)^6$$

where l is the nearest-neighbor spacing. The three methods give the following results for the bcc phase:

$$J=0.42\omega_e \text{ [BPP and observed } (\tau_{ZL})_{\rm min}\text{]},$$

$$J=0.38\omega_e \text{ [Torrey and observed } (\tau_{ZL})_{\rm min}\text{]}.$$

The value of $(\tau_{ZL})_{\rm min}$ used is 60 msec at 4.8 Mc/sec and $V=20$ cm^3. It appears as a cross on Fig. 4.

$$J=0.38\omega_e \text{ [Torrey, using his calculated } (\gamma H_{\rm loc})^2\text{]}.$$

Hartmann obtained $J=0.42\omega_e$ by calculation using $[g(\tau)]_{\rm diffusion}=e^{-\tau/\tau_c}$. Garwin and Landesman obtained $J=0.23\omega_e$. We believe this to be due to their assuming $[g(\tau)]_{\rm diff.}=e^{-\tau/\tau_c}$ and comparing the result that this leads to with some results of Torrey who did not assume such a correlation function.

We have used

$$J=(0.40\pm 0.02)\omega_e \text{ bcc phase} \quad (9a)$$

in all this work. A similar argument for the hcp phase leads to,

$$J=(0.32\pm 0.02)\omega_e \text{ hcp phase.} \quad (9b)$$

Putting these values into Eq. (7) gives

$$(1/\tau_{ZX})^{\rm bcc}=[7.3\times 10^{10}/JV^2][\exp(-\omega_0^2/12.5J^2)+4\exp(-\omega_0^2/3.1J^2)], \quad (10a)$$

$$(1/\tau_{ZX})^{\rm hcp}=[5.8\times 10^{10}/JV^2][\exp(-\omega_0^2/19.0J^2)+4\exp(-\omega_0^2/4.7J^2)]; \quad (10b)$$

V is the molar volume of the sample in cm^3, τ_{ZX} is in sec, and J and ω_0 are in sec^{-1}.

In Fig. 5, $\ln\tau_{ZX}$ is plotted against f_0^2, where $f_0=\omega_0/2\pi$ is the resonance frequency. The full line labeled τ_{ZX} is obtained from Eq. (10a), with $V=20$ cm^3 and $J/2\pi=1$ Mc/sec. The line labeled τ_2 is the expected value of the transverse relaxation time (not measured in this work). For $f_0\gg J/2\pi$ it has the value $(\tau_2)_\infty$ given by Eq. (8), and as $(2\pi f_0/J)$ approaches zero it tends to $(\tau_2)_0=0.3(\tau_2)_\infty$ due to the "10/3 effect" discussed by Kubo and Tomita.[9]

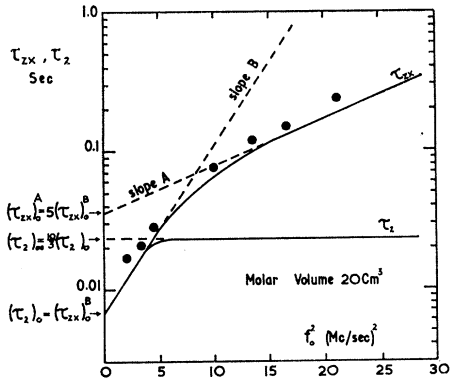

FIG. 5. The frequency variation of the Zeeman-exchange relaxation time τ_{ZX}, and the transverse relaxation time τ_2, in solid He^3 of molar volume 20 cm^3 at a temperature of 1°K.

To obtain J values from Eq. (10), we measure τ_{ZX} as a function of frequency. We must ensure that we are in the temperature-independent region of Fig. 4. This can be found by cooling from the melting line with a highly saturating rf voltage applied to the coil. The signal size, continuously monitored on a chart recorder, then measures τ_1 and when it becomes constant (apart from the relatively slow variation as $1/T$ from Curie's Law), measurements of τ_{ZX} are made starting at the highest frequency. After the measurements at the lowest frequency have been completed, the temperature is lowered to check that the recoveries are still characterized by τ_{ZX} (i.e., are still in the temperature-independent region). The results for molar volume 20 cm^3 are plotted in Fig. 5. The points clearly show the change in slope resulting from the presence of two terms in Eq. (10a) but they fall about 20% high, presumably because of the various approximations made in deriving Eqs. (10). It is impossible to improve the fit for all points by choosing a different value of J.

This was the only molar volume where the results showed this change of slope. The other results are plotted in Fig. 6 with points given for only two molar volumes for the sake of clarity. As shown in Fig. 5, a plot of $\ln\tau_{ZX}$ against f_0^2 will be asymptotic to two straight lines of different slope at high and low frequencies. At sufficiently high frequencies we may neglect the second term in Eqs. (10) and obtain for the bcc phase

$$1/\tau_{ZX}=[7.3\times 10^{10}/JV^2]\exp(-\omega_0^2/12.5J^2), \quad (11a)$$

[9] R. Kubo and K. J. Tomita, J. Phys. Soc. Japan **9**, 888 (1954). Richardson, Meyer, and Hunt at Duke University have recently observed the "10/3 effect" in solid He^3. We are grateful to Dr. H. Meyer for making available to us a paper scheduled for publication.

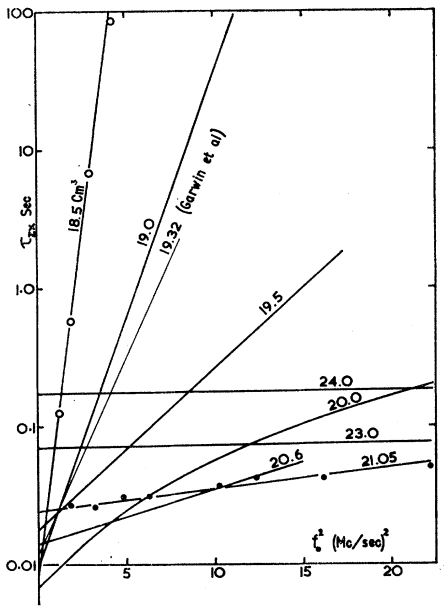

FIG. 6. The frequency variation of the Zeeman-exchange relaxation time τ_{ZX} in solid He^3 at various molar volumes marked on the curves.

which is the line of slope A in Fig. 5. For the hcp phase

$$1/\tau_{ZX}=[5.8\times10^{10}/JV^2]\exp(-\omega_0^2/19.0J^2). \quad (12a)$$

At sufficiently low frequencies we may use the approximation $e^{-x}+4e^{-4x}\approx5-17x\approx5e^{-17x/5}$ for $x\ll1$, to obtain for the bcc phase

$$1/\tau_{ZX}=[3.6\times10^{11}/JV^2]\exp(-\omega_0^2/3.7J^2), \quad (11b)$$

which is the line of slope B. For the hcp phase

$$1/\tau_{ZX}=[2.9\times10^{11}/JV^2]\exp(-\omega_0^2/5.6J^2). \quad (12b)$$

From the fact that all the results in Fig. 6 (except for molar volume 20 cm^3) do give straight lines, we may assume that either Eqs. (11) or (12) are applicable. We obtain two values of J from each of Eqs. (11) and (12), one value from the slope, and one from the intercept. We can distinguish which is the appropriate equation by which gives better internal agreement for the two values. If we use the wrong equation we shall get a value of J from the intercept wrong by a factor of 5, but a value from the slope wrong by a factor of only 1.8. Hence we will get an internal disagreement by a factor of about 3. Table I gives values of J calculated from Eqs. (11) and (12) in this way, called J^τ in this work. The parameters $(\tau_{ZX})_0$ and f_e arise from fitting the straight lines of Fig. 6 to the equation $\tau_{ZX}=(\tau_{ZX})_0\times\exp(f_0^2/f_e^2)$. We find that for the hcp phase, Eq. (12a) is correct for our range of frequencies. If for instance we apply Eq. (12b) to the results for molar volume 19 cm^3, we would obtain a $J/2\pi$ from $(\tau_{ZX})_0$ of 1.3 Mc/sec and a value from f_e of 0.51 Mc/sec. For most of the bcc phase, Eq. (11b) is found to give good internal consistency as shown. The results for molar volume 20 cm^3 cannot be fitted to a straight line because neither approximation used in setting up Eqs. (11a) and (11b) can be employed and we have to use the full Eq. (10a).

Table I also gives some other values of τ_{ZX} which are not extensive enough to plot on Fig. 6 but can be used to obtain values of J. Where two values of τ_{ZX} are available at a given molar volume, J is calculated from the ratio of the two values using Eq. (10). J^τ values from Table I are plotted in Fig. 12.

Hartmann[6] interpreted Reich's τ_{ZX} measurements[10] on the basis of an equation similar to 10a but since the results were only at one frequency, the J values derived are not very accurate, particularly as the values of ω_0 and J available were in a region where the J values are very strongly dependent on the exact values of the constants in Eq. (10a).

D. Exchange-Lattice Relaxation Time

Garwin and Landesman[1] first suggested mechanisms coupling the exchange and lattice together. We believe we have observed two of the types of coupling that they discussed.

1. Coupling to the Phonons

The exchange interaction varies very rapidly with interatomic spacing, and the lattice vibrations thus modulate very strongly the interaction between neighboring pairs of spins. This leads to a coupling between the exchange and lattice baths which has been discussed in detail by Griffiths.[11] Two types of process may be effective, one in which a single phonon is concerned and a second in which one phonon is absorbed by the exchange system and another phonon of different energy is created. Griffiths has calculated the coefficients for the two processes and his results, modified so as to apply to He^3, become

$$(1/\tau_{XL})_{1\text{ phonon}}=k_1J^2J'^2T/\Theta^5\ \text{sec}^{-1},$$
$$k_1=3.0\times10^{-45}\ \text{bcc phase}=7.9\times10^{-45}\ \text{hcp phase}, \quad (13)$$

$$(1/\tau_{XL})_{2\text{ phonon}}=k_2J''^2T^7/\Theta^{10}\ \text{sec}^{-1},$$
$$k_2=2.6\times10^{-35}\ \text{bcc phase}=4.6\times10^{-35}\ \text{hcp phase}, \quad (14)$$

where $J'\equiv\partial J/\partial a$, $J''\approx\partial^2J/\partial a^2$, a is the lattice spacing in cm, and Θ is the Debye temperature. The last equation is similar to one derived by Garwin and Landesman from Griffiths' work, but the coefficient is a factor of three larger since Garwin and Landesman used one of

[10] H. A. Reich, Phys. Rev. **129**, 630 (1963).
[11] R. B. Griffiths, Phys. Rev. **124**, 1023 (1961).

TABLE I. Values of the exchange integral J calculated from Zeeman-exchange relaxation times τ_{ZX} measured at different resonance frequencies f_0. Except as indicated, values are obtained by fitting results to $\tau_{ZX}=(\tau_{ZX})_0 \exp(f_0^2/f_e^2)$ and comparing $(\tau_{ZX})_0$ and f_e obtained with Eqs. (11) and (12).

Molar volume (cm³)	$(\tau_{ZX})_0$ (msec)	$J/2\pi$ from $(\tau_{ZX})_0$ (Mc/sec)	f_e (Mc/sec)	$J/2\pi$ from f_e (Mc/sec)	$J^\tau/2\pi$ (Mc/sec)	Equation used	Notes
hcp phase							
18.5[a]	8±2	0.22±0.05	0.67±0.03	0.16±0.01	0.17±0.02	(12a)	
19.0	10±1	0.26±0.03	1.13±0.04	0.26±0.01	0.26±0.02	(12a)	
19.32	12±1	0.30±0.3	1.50±0.2	0.35±0.02	0.33±0.02	(12a)	These figures are from Garwin and Landesman.[1]
19.4	···	···	···	···	0.38±0.04	(10b)	J^τ derived from $\tau_{ZX}^{-1}=0.06$ sec^{-1}, $f_0^2=19.0$ (Mc/sec)²
19.5	18±1	0.44±0.03	1.95±0.04	0.45±0.01	0.44±0.02	(12a)	
19.6	···	···	···	···	0.50±0.04	(10b)	J^τ derived from $\tau_{ZX}^{-1}=0.4$ sec^{-1}, $f_0^2=22.5$ (Mc/sec)²
bcc phase							
19.75	···	···	···	···	1.17±0.1	(10a)	J^τ derived from $\tau_{ZX}^{-1}=75$ and 2.3 sec^{-1}, $f_0^2=2$ and 23 (Mc/sec)²
20.0	The points for this molar volume do not fall on a straight line (see Fig. 6)				1.21±0.1	(10a)	J^τ derived from $\tau_{ZX}^{-1}=30$ and 4 sec^{-1}, $f_0^2=4.8$ and 23 (Mc/sec)²
20.6	14±2	1.9 ±0.2	3.30±0.2	1.7 ±0.1	1.8 ±0.1	(11b)	
21.05	24±2	3.1 ±0.3	5.2 ±0.3	2.7 ±0.2	2.9 ±0.4	(11b)	
22.05	36±5	4.3 ±0.6	···	···	4.3 ±0.6	(11b)	The results here had too large a scatter to determine a slope.
23.0	70±0	7.7 ±1.0	13.4 ±2.0	7.0 ±1.0	7.4 ±1.0	(11b)	
24.0	170±10	17.0 ±1.0	···	···	17.0 ±1.0	(11b)	

[a] All molar volumes are estimated to be correct to within 0.05 cm³.

Griffiths' approximations which is not required for the case of He³.[12]

2. *Coupling via Diffusion*

The short range of the exchange forces means that the exchange energy of a spin on one lattice site is uncorrelated with its energy after it has diffused to a neighboring site. Lattice jumps are thus a mechanism for relaxing the exchange energy which leads to a τ_{XL} of about τ_c, the jump time in the solid. We can relate τ_c to the macroscopic diffusion coefficient through $\tau_c=a^2/6D$.

In general, we may expect the transition probabilities for the processes discussed above to add giving,

$$(1/\tau_{XL})_{\text{observed}}=(1/\tau_{XL})_{1\text{ phonon}}+(1/\tau_{XL})_{2\text{ phonon}}+6D/a^2. \quad (15)$$

The three processes can be distinguished by their temperature dependence which is, respectively, T, T^7, and $e^{-\theta/T}$ with $\theta\approx 10$°K for the bcc phase.[10]

Actually, we cannot observe τ_{XL} directly because it is the characteristic time with which the exchange bath would relax to the lattice if the former were uncoupled from the Zeeman system. Since we can only observe the Zeeman system recovering, we use the fact that when it is well coupled to the exchange bath it recovers with a time constant $\tau_{XL}(1+k_Z/k_X)$, where k_Z/k_X is the ratio of the specific heats of Zeeman and exchange baths when they are at the same temperature. This result is proved in Sec. IIIE. In order to obtain τ_{XL}, we must either know k_Z/k_X or by working as a function of frequency ($k_Z\propto f_0^2$) extrapolate to $k_Z=0$. In general, the latter method is used and, as discussed in the next section, it is also used to obtain k_X.

Figure 7 gives the results for τ_{XL} as a function of temperature for several molar volumes in each phase. To reduce confusion, experimental points are again plotted for only two molar volumes. The scatter of points on all the other curves is similar. The slopes of the straight line portions of the curves give $\tau_{XL}\propto T^{-n}$ in these regions with $6.7<n<7.8$ in all cases. This is taken as strong support for the two-phonon process being the dominant exchange-lattice coupling mechanism in this region. The result of Garwin and Reich[3] is also shown. It lies about 100 times above our values. We believe they were in fact not measuring τ_{XL}, but a further relaxation time which we discuss in Sec. IV caused by the presence of He⁴ impurity.

In PRL,[2] we plotted the results in the form $\ln\tau_{XL}$ against $1/T$ and deduced that $\tau_{XL}\propto e^{\Delta/T}$. Working over a limited temperature range, it is difficult to distinguish between an exponential dependence and a power law, but there is no doubt that, with the more extensive data now available, the power law gives a better fit.

In the hcp phase all the points appear to obey a T^{-7} law but, in the bcc phase, there are departures at low and high temperatures. In Fig. 8 is plotted the value of $(\tau_{XL})_{2\text{ phonon}}$ at a temperature of 0.5 °K as a function of

[12] We are grateful to Dr. P. M. Richards, for pointing this out to us. In a paper to be published, he has extended Griffiths' theory to account for correlations between pairs of exchange-coupled spins. In the case of a 3-dimensional lattice however, this only changes the coefficients in Eqs. (13) and (14) by about 20%.

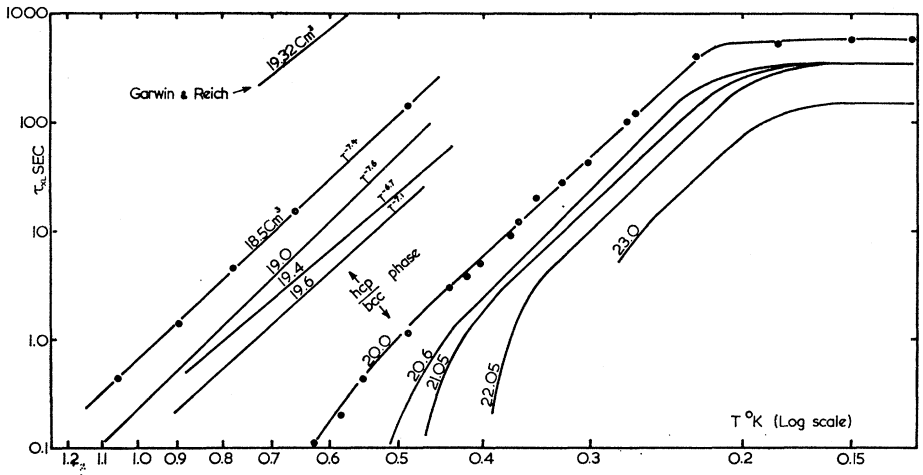

FIG. 7. The temperature variation of the exchange-lattice relaxation time τ_{XL} in solid He^3 at various molar volumes marked on each curve. A straight line indicates $\tau_{XL} \propto T^{-n}$ and values of n are given for the hcp phase.

molar volume. This is done for the bcc phase by extrapolating the straight line portions in Fig. 7 to 0.5 °K. The purpose is to check the agreement with Griffiths' theory. The molar-volume dependence in Griffiths' results is due to the factor J''^2/Θ^{10} in Eq. (14). We find that the observed dependence of τ_{XL} appears to be very roughly as Θ^{10}, suggesting that J''^2 is not a very strong function of molar volume. For this reason J'' has been calculated from the observed variation of J with a by fitting to a curve of the type

$$J = pa^2 + qa + r \qquad (16)$$

giving $J'' = 2p$. p, q and r are obtained by fitting three smoothed points read off Fig. 12 to Eq. (16). This leads to

$$J''/2\pi = 380 \pm 80 \text{ Mc/sec Å}^{-2} \text{ bcc phase},$$
$$J''/2\pi = 130 \pm 40 \text{ Mc/sec Å}^{-2} \text{ hcp phase}.$$

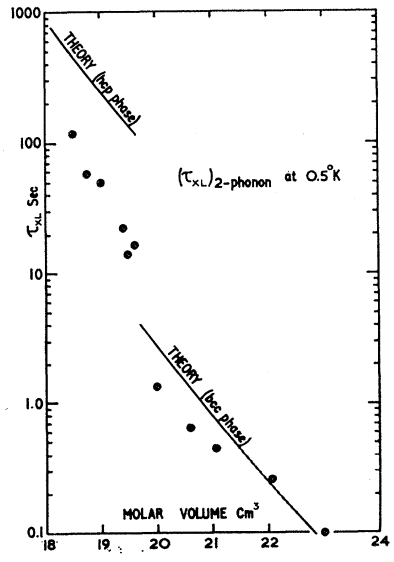

FIG. 8. The molar volume variation of the exchange-lattice relaxation time due to the 2-phonon process at a temperature of 0.5°K.

The "theory" lines in Fig. 8 have been calculated from Eq. (14) using these values for J'' and published data for Θ.[13] The fit is quite good considering the approximations made in Griffiths' theory and also the assumption that the J'' required in Eq. (14) is that obtained by measuring J as a function of molar volume.

Figure 8 also shows the bcc-hcp phase boundary where there is a discontinuity in τ_{XL} of a factor of about 7.

In the bcc phase, Fig. 7 shows τ_{XL} departing from a T^{-7} law. In particular we may note:

(1) At high T, τ_{XL} falls below a T^{-7} law. If we suppose this to be due to diffusion providing an extra mechanism for exchange-lattice coupling, we may use Eq. (15) to derive values of the diffusion coefficient. Figure 9 gives the D values so derived.

The lines in the graph are obtained by extrapolating Reich's[10] results using his smoothed values for the activation energy. The thickened region indicates where Reich actually determined values of D. The good fit of the lines strongly suggests that diffusion is the mechanism causing τ_{XL} to fall below the T^{-7} line in Fig. 7.

Actually, Reich found that at low enough temperatures, D became constant at values of about 10^{-8} $cm^2\ sec^{-1}$; he suggested this was due to the exchange process contributing to diffusion, on the grounds that spin diffusion and atomic diffusion are indistinguishable.

Edwards *et al.*[14] in reporting the solid He^3-He^4 phase separation found that the relaxation time associated with the specific heat anomaly was about 15 sec at molar volume 23.9 cm^3. This in itself is not inconsistent with our observations since this would be the expected time for a He^3 atom to move as much as 100 Å at 0.2 °K and at this molar volume.[15] What is not clear is why

[13] E. C. Heltemes and C. A. Swenson, Phys. Rev. **128**, 1512 (1962).

[14] D. O. Edwards, A. S. McWilliams, and J. G. Daunt, Phys. Letters **1**, 218 (1962).

[15] This estimate comes from assuming $D = D_0 \exp(-\theta/T)$ and $\tau = a^2/6D$ and obtaining D_0 and θ from extrapolating Reich's results.

the time should be independent of the temperature at which the anomaly occurs. (This varies with the He^3-He^4 concentration.)

(2) At low temperatures, the relaxation time becomes almost constant. Also, below about 0.3 °K, the recoveries were invariably nonexponential. A faster recovering term appears at about 0.3 °K and increased in importance until at 0.1 °K the recovery can be described by the sum of two exponential terms with approximately equal coefficients. The shorter relaxation time is about one tenth as long as the one plotted in Fig. 7.

While we have no complete explanation for these effects, we believe they could be related to the fact that the lattice specific heat is small at low temperature, and in fact we expect the exchange and spin specific heat to equal the lattice specific heat at about 0.1 °K in the bcc phase. If the lattice is not well coupled to its surroundings or if there is a phonon bottleneck problem, nonexponential recoveries could occur. Also, an apparent temperature independence of τ_{XL} might result from heating of the lattice as the magnetic baths deliver their energy into it.

We may note that this near constancy of τ_{XL} cannot be due to the single-phonon process becoming the dominant one because of the very strong molar volume dependence involved in $J^2J'^2/\Theta^5$ [see Eq. (13)] whereas Fig. 7 shows that there is relatively little dependence on molar volume.

E. The Exchange Specific Heat and the Rate Equations

Before discussing the rate equations we first obtain expressions for the Zeeman and exchange-bath energies and specific heats. Writing the spin Hamiltonian,

$$\mathcal{H}_{\text{spin}}=\mathcal{H}_0+\mathcal{H}_X,$$

where

$$\mathcal{H}_0=\gamma\hbar H_0\sum_{i=1}^{N} I_z^i,$$

and

$$\mathcal{H}_X=\tfrac{1}{2}\hbar J\sum_{i\neq j}{}' \mathbf{I}^i\cdot\mathbf{I}^j.$$

($\sum'$ means sum over nearest neighbors only.) For high temperatures where $kT\gg\hbar J$, $\hbar\gamma H_0$, the density matrix may be written

$$R=([1]-\beta\mathcal{H})/\mathrm{tr}[1], \quad \text{where} \quad \beta=1/kT.$$

For the energy of the system, we may write

$$E=\mathrm{tr}[R\mathcal{H}].$$

A straightforward calculation leads to

$$E=E_Z+E_X,$$

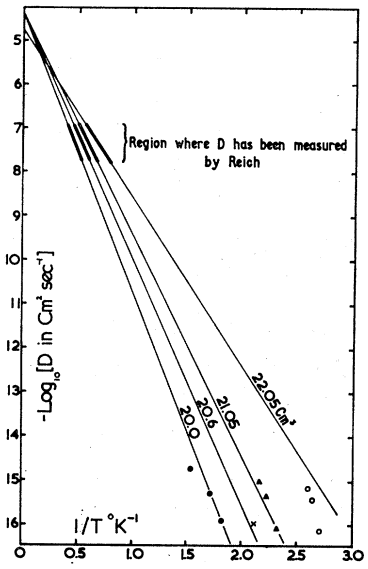

FIG. 9. The temperature variation of the diffusion coefficient, D in solid He^3 at various volumes marked on each line. The lines are extrapolations of Reich's (Ref. 10) data using his smoothed values for the activation energy.

where

$$E_Z=-N(\hbar\gamma H_0)^2/4kT_Z\equiv -k_Z/T_Z,$$

and (17a)

$$E_X=-3Nz(\hbar J)^2/32kT_X\equiv -k_X/T_X,$$

giving

$$C_Z=k_Z/T_Z^2 \quad \text{and} \quad C_X=k_X/T_X^2; \tag{17b}$$

z is the number of nearest neighbors.

These values are written into the baths in Fig. 3. One of the chief inconsistencies in earlier work[1,3] on the magnetic properties of solid He^3 was the large discrepancy between observed values of C_X and values calculated from Eq. (17b). As explained earlier, the recoveries from saturation will always be exponential, with time constant τ_{ZX}, if the specific heat of the exchange bath is large enough or the coupling of the exchange to the lattice is strong enough. Previous workers[10,1] found the recoveries always to be characterized by τ_{ZX} (i.e., temperature-independent) though they came to different conclusions as to why this was so. More recently Garwin and Reich[3] were able to measure the exchange-bath specific heat by applying rf heating to the Zeeman system when the exchange was almost uncoupled from the lattice. They found a value about 4000 times larger than that calculated from their J values. We shall discuss this later and suggest that it was due to the presence of about 1% He^4 impurity.

The starting point for a derivation of the rate equations is the Bloch equations for the Zeeman and exchange baths. Subscripts Z and X will be used to specify the Zeeman and exchange baths, respectively.

For the Zeeman system in the absence of an applied rf

field, we have

$$dM_Z/dt=(M_X-M_Z)/\tau_{ZX}. \tag{18}$$

In this and subsequent equations M always means the component of **M** parallel to the dc magnetic field, and a symbol like M_X means the value this component of **M** would have if the spin temperature were equal to T_X.

Provided $kT_L\gg\hbar J$, $\hbar\gamma H_0$ we can write $M_i\propto 1/T_i$.

For convenience we define

$$Z\equiv T_L/T_Z,\quad X\equiv T_L/T_X,\quad \text{and}\quad \eta_1\equiv(\tau_{ZX})^{-1}$$

where T_L is the lattice temperature.

Equation (18) now becomes

$$dZ/dt=\eta_1(X-Z).$$

The effect of the applied rf field can be found in terms of W, the probability per unit time for induced transitions.

$$(dM/dt)_W=(n_+-n_-)Wm=-WM,$$

n_+ and n_- are the number of spins pointing with and against the dc field, and m is the magnetic moment per spin.

The full rate equation for the Zeeman system now becomes

$$dZ/dt=\eta_1(X-Z)-WZ.$$

A similar expression can be written for the exchange bath,

$$dX/dt=\eta_2(1-X)+\rho\eta_1(Z-X), \tag{19}$$

where the second term accounts for the effect of quanta coming from the Zeeman bath and $\eta_2\equiv(\tau_{XL})^{-1}$. To calculate ρ we use the requirement of conservation of energy in the absence of any coupling of the exchange to the lattice or of any rf field. This gives

$$C_Z dT_Z/dt+C_X dT_X/dt=0,$$

i.e.,

$$C_Z T_Z^2 dZ/dt+C_X T_X^2 dX/dt=0,$$

and therefore

$$k_Z\eta_1(X-Z)+\rho\eta_1 k_X(Z-X)=0,$$

giving $\rho=k_Z/k_X$ with k_Z and k_X given by Eq. (17a). Equations (18) and (19) are used to solve for Z and X giving:

$$Z=Z_\infty+Ce^{-\lambda_1 t}+De^{-\lambda_2 t}, \tag{20}$$

where

$$Z_\infty=\eta_1\eta_2/[\eta_1\eta_2+W(\rho\eta_1+\eta_2)], \tag{21}$$

$$\lambda_1=\tfrac{1}{2}[(1+\rho)\eta_1+\eta_2+W]+\tfrac{1}{2}[(W-(\rho-1)\eta_1-\eta_2)^2+4\rho\eta_1^2]^{1/2}, \tag{22a}$$

$$\lambda_2=\tfrac{1}{2}[(1+\rho)\eta_1+\eta_2+W]-\tfrac{1}{2}[(W-(\rho-1)\eta_1-\eta_2)^2+4\rho\eta_1^2]^{1/2}, \tag{22b}$$

$$\frac{C}{D}=\frac{(\eta_1+W-\lambda_2)(Z_0-Z_\infty)-\eta_1(X_0-X_\infty)}{\eta_1(X_0-X_\infty)-(\eta_1+W-\lambda_1)(Z_0-Z_\infty)}; \tag{23}$$

and

$$X=X_\infty+Pe^{-\lambda_1 t}+Qe^{-\lambda_2 t}, \tag{24}$$

where

$$X_\infty=\eta_2(W+\eta_1)/[\eta_1\eta_2+W(\rho\eta_1+\eta_2)], \tag{25a}$$

$$P/Q=(C/D)(W+\eta_1-\lambda_1)/(W+\eta_1-\lambda_2); \tag{25b}$$

X_0 and Z_0 are the values of X and Z at time zero.

An examination of Eqs. (22) and (23) shows that the equations are greatly simplified if $\eta_2/\rho\gg\eta_1\gg W$ or $\rho\eta_1\gg\eta_2\gg W$. In the former case we obtain

$$Z=Z_\infty-(Z_\infty-Z_0)e^{-\eta_1 t}, \tag{26}$$

and in the latter

$$Z=Z_\infty-(Z_\infty-Z_0)e^{-\eta_2 t/(1+\rho)}. \tag{27}$$

These equations confirm that if the exchange bath is well coupled to the lattice, the recoveries have the characteristic time τ_{ZX} and if the Zeeman and exchange baths are well coupled, the characteristic time of recovery is $\tau_{XL}(1+\rho)$. These two conditions define, respectively, regions I and III of Fig. 4.

The latter case provides a method for measuring the exchange-bath heat capacity. If, in the region $\rho\tau_{XL}\gg\tau_{ZX}$, we plot recovery times [i.e., $(\lambda_2)^{-1}$] as a function of frequency, we can obtain the exchange heat capacity through Eqs. (17):

$$\rho\equiv k_Z/k_X=C_Z/C_X=(8/3z)(2\pi f_0/J)^2.$$

The second equality assumes $T_X=T_Z$ which is already implied by the condition $\rho\tau_{XL}\gg\tau_{ZX}$.

Figure 10 shows such a plot for molar volume 20 cm³. The intercept on the f_0^2 axis is $-(3z/8)(J/2\pi)^2$ and that on the time axis is the value of τ_{XL} at the temperature concerned. It is in this way that the values of τ_{XL} plotted in Fig. 7 were obtained. It was possible to obtain values of J in this way for all molar volumes up to 22 cm³. Above this, the limited variation in $(1+\rho)$ available with our frequency range required a different technique to be devised.

By working at a low temperature where τ_{XL} was about 100 sec and τ_{ZX} about 0.1 sec, we were able to put controlled amounts of rf heating into the Zeeman system

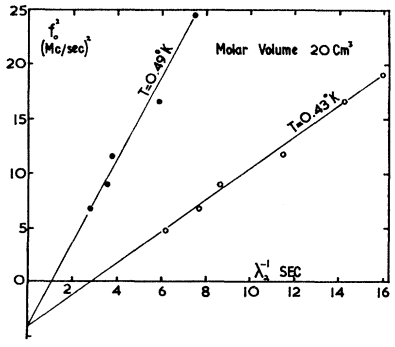

FIG. 10. The frequency variation of the characteristic recovery time of the Zeeman and exchange baths in region III of Fig. 4.

and watch how much the Zeeman and exchange baths warmed as a result.

With $\eta_2=0$, Eq. (19) gives

$$\Delta X=\rho(Z_0-X_{\text{mean}})\tau/\tau_{ZX}; \tag{28}$$

Z_0 corresponds to the temperature of the Zeeman system while the rf heating is being applied for a time τ. X_{mean} corresponds to the exchange bath temperature which changes by ΔX due to energy coming from the Zeeman bath. The envelope of an observed recovery will be as in Fig. 11. Because of the proportionality of $Z(=T_L/T_Z)$ to the signal height observed on the oscilloscope, Eq. (28) may be written

$$\Delta h=\rho(h_{\text{mean}}-h_0)\tau/\tau_{ZX}.$$

The heights are defined from Fig. 11. h_0 is the signal height with low rf voltage extrapolated back to $t=\tau$.

We have not yet discussed the case of $\rho\eta_1\approx\eta_2$. This is particularly interesting because we can no longer neglect C or D in Eq. (20) and the recoveries will be nonexponential. Also, we may use the observed ratio of C/D to obtain a value for ρ, and hence for the exchange-bath specific heat.

To simplify the computation, two extreme sets of starting conditions have been used. In the first the initial saturation is carried out in a time so short that the exchange bath is insignificantly heated before the recovery starts. This is equivalent to writing $X_0=X_\infty$ in Eq. (23). We can now obtain η_1, η_2, and ρ in terms of the 3 observables λ_1, λ_2, and C/D. The calculation gives, assuming $W\ll\eta_1$,

$$\eta_1=\tau_{ZX}^{-1}=\lambda_1(C/D+\lambda_2/\lambda_1)/(1+C/D), \tag{29a}$$

$$\eta_2=\tau_{XL}^{-1}=\lambda_2(1+C/D)/(C/D+\lambda_2/\lambda_1), \tag{29b}$$

$$\rho=(C/D)(1-\lambda_2/\lambda_1)^2/(C/D+\lambda_2/\lambda_1)^2. \tag{29c}$$

The procedure is to fit an observed recovery to

$$h=h_\infty+h_Ce^{-\lambda_1 t}+h_De^{-\lambda_2 t}$$

and calculate τ_{ZX}, τ_{XL} and ρ from Eq. (29). Figure 3A of PRL shows such a recovery for solid He^3 with $\frac{1}{2}\%$ He^4. As mentioned in PRL, we were also able to observe nonexponential recoveries at several molar volumes in the pure solid.

An alternative simple set of starting conditions for a recovery is obtained if we apply a highly saturating rf voltage to the system for a time long enough for all the baths to come to equilibrium. In this case we have to

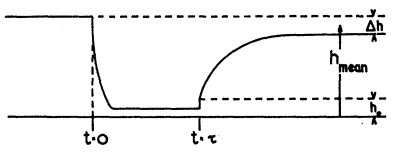

FIG. 11. The envelope of the signal "spikes" during a measurement of the exchange bath specific heat by applying a pulse of high rf power between $t=0$ and $t=\tau$.

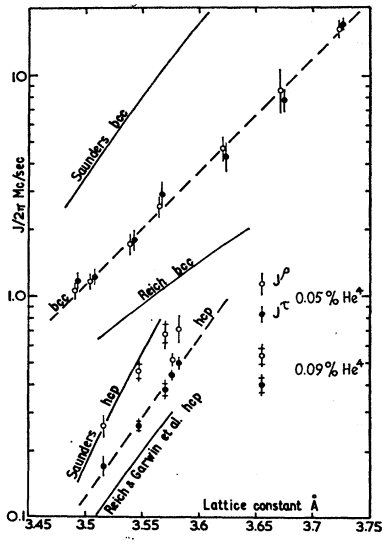

FIG. 12. The variation with interatomic spacing of the exchange integral J. The experimental results of Reich (Ref. 10) and Garwin and Landesman (Ref. 1), and the theoretical curves due to Saunders (Ref. 16) are taken from Garwin and Landesman's paper.

apply Eqs. (20) and (24) to find the starting conditions (i.e., X_0 and Z_0) and then apply Eq. (20) to the recovery. The results are identical to Eq. (29) except that λ_1C/λ_2D replaces C/D, and they are independent of the exact high rf field applied. Figure 3(b) of PRL gives a recovery of this kind. The values of ρ, τ_{ZX}, and τ_{XL} calculated from the two recoveries agree to within 20%.

J values calculated by any of the three methods described in this section are called J^ρ to distinguish them from values obtained from τ_{ZX}. Both sets of J values are recorded in Table II and plotted in Fig. 12, together

TABLE II. Values of J^ρ, the exchange integral calculated from measurements of the exchange specific heat. Unless otherwise noted, J^ρ is obtained from the relation $(3z/8)(J^\rho/2\pi)^2=F^2$, where F^2 is the intercept on the negative f_0^2 axis in plots of λ_2^{-1}, the recovery time of the Zeeman and exchange baths to the lattice, against f_0^2. z is the number of nearest neighbors in the crystal and f_0 is the resonance frequency. The He^4 content is 0.05% except as noted.

Molar volume (cm^3)	Lattice spacing (Å)	F^2 $(Mc/sec)^2$	$J^\rho/2\pi$ (Mc/sec)	$J^\tau/2\pi$ (Mc/sec)
hcp phase				
18.5	3.515	0.31±0.07	0.26±0.03	0.17±0.02
19.0	3.546	0.95±0.20	0.46±0.05[a]	0.26±0.02
19.4	3.571	2.1 ±0.6	0.68±0.10[a]	0.38±0.04
19.5	3.577	1.2 ±0.2	0.52±0.04	0.44±0.02
19.6	3.583	2.2 ±0.6	0.71±0.10	0.50±0.04
bcc phase				
19.75	3.492	3.5 ±0.6	1.08±0.10	1.17±0.10
20.0	3.507	4.2 ±0.35	1.2 ±0.10	1.21±0.10
20.6	3.542	9.7 ±2.0	1.8 ±0.2	1.8 ±0.2
20.6	3.542	···	1.8 +0.1[b]	1.8 ±0.2
21.05	3.567	20 ±4	2.6 ±0.3	2.9 ±0.4
21.05	3.567	···	3.4 ±0.5[b]	2.9 ±0.4
22.05	3.623	70 ±18	4.8 ±0.6	4.3 ±0.6
23.0	3.674	···	9.0 ±2.0[c]	7.7 ±1.0
24.0	3.727	···	17.0 ±1.0[c]	17.0 ±1.0

[a] These samples contained 0.09% He^4.
[b] Results obtained from analysis of nonexponential recoveries.
[c] Results obtained by applying rf heating pulses to Zeeman system.

TABLE III. Values of J^ρ, the exchange integral calculated from measurements of the exchange specific heat, for samples containing 0.5% He^4.

Molar volume (cm^3)	$J^\rho/2\pi$ (Mc/sec)	$J^\tau/2\pi$ for pure[a] He^3 (Mc/sec)	$[(J^\rho)^2-(J^\tau)^2]^{1/2}/2\pi$ (Mc/sec)
hcp phase			
18.4	2.3±0.3[b]	0.15	2.3±0.3
19.0	2.3±0.4[c] 2.9±0.2[b]	0.27	2.7±0.3
19.6	2.8±0.4[b] 2.7±0.4[c]	0.50	2.7±0.3
bcc phase			
20.0	3.1±0.3[b]	1.3	2.8±0.3

[a] Smoothed results from Fig. 12 are used.
[b] Results obtained from analysis of nonexponential recoveries.
[c] Results obtained from frequency dependence of observed recoveries.

with those given by other workers and by the theory due to Saunders.[16]

The agreement between J^ρ and J^τ in the bcc phase is extremely good. In the hcp phase, the J^ρ values are systematically higher. This we believe to be due to the presence of 0.05% or 0.09% He^4, an effect to be discussed further in Sec. IV. It is shown there that the He^4 impurity appears to add a constant amount to $(J^\rho)^2$ and hence we would not expect the discrepancy to be detectable in the bcc phase where J is several times greater.

IV. RESULTS IN IMPURE He^3

As mentioned earlier, our first measurements were made on samples containing 0.5% He^4. By comparison with the results for purer samples, we may make the following observations.

The Zeeman-exchange relaxation time is not greatly affected. More precisely, Eq. (10) is obeyed with k_2J^2 substantially unchanged and k_1/J reduced by a factor of less than two compared with the purer sample at the same density. This suggests that few pair interactions in the sample are strongly affected by the He^4. On the other hand, the exchange-bath heat capacity appears to be greatly increased. Table III gives the values of J^ρ for four molar volumes with values of J^τ in pure He^3 given for comparison. Most of the J^ρ results come from an analysis of nonexponential recoveries with a few others from the frequency variation of the recovery of the combined Zeeman and exchange system. The large increase in J^ρ together with the much smaller change in the Zeeman-exchange recovery times suggests that the He^4 might be locally increasing the exchange interaction by a large factor, leaving the bulk of the sample unaffected. If we write the total exchange energy as the sum of two contributions

$$E_X=(E_X)_{\text{bulk}}+(E_X)_{\text{impurity}},$$

hence

$$J^2=(J^2)_{\text{bulk}}+(J^2)_{\text{impurity}}.$$

The last column in Table III shows that $(J)_{\text{imp}}$ is substantially independent of molar volume and equal to about 2.7 Mc/sec per atom. If we suppose that the local increase in J is due to changing nearest-neighbor spacing, we can calculate what local strain would be required to explain the results. For this purpose we suppose that it is only the nearest neighbors of an He^4 atom that contribute to the term $(J^2)_{\text{imp}}$. In this case the local value of J must be greater than 2.7 Mc/sec by a factor $(200/12)^{1/2}$ since 1 in 200 atoms are He^4 and there are 12 nearest neighbors in the hcp phase. This leads to a local J of about 11 Mc/sec which is the bulk value to be expected at a lattice spacing of about 3.75 Å if we extrapolate the J^τ results in Fig. 12. This corresponds to a local linear strain of about 5%. Klemens *et al.*[17] have calculated a 5% volume strain for He^4 in He^3. Another estimate can be obtained from the difference in the molar volumes of solid He^3 and He^4 at the same pressure.[18] This leads to a figure of about 7% for the volume strain.

In He^3 containing $\frac{1}{2}$% He^4, the relaxation behavior can be described by the three-bath model only down to a temperature around 0.7 °K, below which both in the approach to saturation (i.e., after applying a high rf field) and in the recovery a third long relaxation time appears. The recoveries can be accurately fitted to an equation of the type

$$h_\infty-h=h_Ce^{-\lambda_1 t}+h_De^{-\lambda_2 t}+h_Ee^{-\lambda_3 t},$$

where the three terms can easily be distinguished because of the large difference in the λ's.

This suggests that the results could be analyzed in terms of four baths in series, though other interpretations are possible. If we suppose that the new bath appears between the exchange bath and the lattice (and is not detectable above 0.7 °K because it is then effectively well coupled to the lattice), its specific heat is 200 times the Zeeman specific heat at 2 Mc/sec and molar volume 19 cm^3. We have no explanation to give for this new heat reservoir but would like to point out that both from the specific heat and the coupling to the lattice we believe that it is the bath that Garwin and Reich[3] observed and called the exchange bath. Their sample was found to contain about 1% He^4. Possibly this bath could account for the high-temperature tail of the specific-heat anomaly associated with the He^3-He^4 phase separation described by Edwards *et al.*,[14] although the value we obtain appears to be an order of magnitude too small.

It seems likely that these results are also relevant to

[16] E. M. Saunders, Phys. Rev. **126**, 1724 (1962).

[17] P. G. Klemens, R. de Bruyn Ouboter, and C. le Pair, Proceedings of the Ninth International Conference on Low Temperature Physics, Columbus, Ohio, 1964 (to be published).

[18] J. Donohue, Phys. Rev. **114**, 1009 (1959).

the early work on the magnetic susceptibility by Adams *et al.*[19] (Hereinafter referred to as AMF) which was at first thought to indicate a large exchange interaction of the order of 0.1°K. Later work on samples in which the He^4 content was reduced to below 0.05% gave only very small departures from Curie's law above 0.06 °K.[20]

The point of interest is whether the early susceptibility measurements were of equilibrium values, in which case the He^4 would have had the remarkable effect of producing appreciable ordering in the solid at 0.2 °K, or whether they were nonequilibrium values because of some long relaxation time. The present measurements suggest that at the temperatures concerned $(\lambda_3)^{-1}$ might be extremely long. The presence of this bottleneck might not be detected by saturation and recovery experiments due to the relatively large heat capacity of the baths interposed between spins and lattice. To try and clarify the matter, we have carried out some susceptibility measurements on samples containing 3% He^4. The difficulty is that below 0.4 °K the lattice temperature cannot be maintained constant indefinitely and it is difficult to distinguish temperature dependence from time dependence. However, we found that Curie's law was obeyed to within about 3% down to 0.1°K at molar volume 22.5 cm^3. At 22 cm^3, large departures of the type found by AMF at similar densities were observed, but whether the susceptibility was above or below the Curie value corresponding to the lattice temperature, the signal was always found to be relaxing towards that value. At molar volume 21.5 cm^3, similar large departures were observed but it was not possible to detect any relaxation proceeding. However, extrapolating the relaxation times observed at molar volumes 22.5 and 22 cm^3, we find that we would not expect to observe any such relaxation, as it would be too slow.

We believe these results to suggest that the "departures from Curie's law" observed by AMF were due to nonequilibrium effects. A curve like the one in their paper labeled "81.6 atm" arises because the spins never cool to the coldest lattice temperature, and on warming up, the lattice "overtakes" the spins, giving an apparent susceptibility *above* the Curie value.

[19] E. D. Adams, H. Meyer and W. M. Fairbank, *Helium Three* (Ohio State University Press, Columbus, Ohio, 1961), p. 57.

[20] A. L. Thomson, H. Meyer, and P. N. Dheer, Phys. Rev. **132**, 1455 (1963).

V. CONCLUSION

Our results above 0.2 °K suggest that the three-bath model gives a self-consistent description for the magnetic relaxation processes occurring in pure solid He^3. Below 0.2 °K further work is required to explain certain features.

Small quantities of He^4 have very marked effects on the relaxation process which can no longer be interpreted fully using the three-bath model. Further work is planned to clarify the position.

ACKNOWLEDGMENTS

We would like to acknowledge the help of many fruitful discussions with Dr. P. M. Richards (in particular the derivation of the rate equations is due to him). We are also indebted to Dr. B. T. Beal for help with experiments and to Dr. K. E. Mayne and Dr. H. Glyde for analysis of He^3-He^4 samples. Dr. D. F. Brewer kindly read through the manuscript and made several helpful suggestions. Grateful acknowledgment is due to the D.S.I.R. and the States of Guernsey for maintenance grants to two of us (M.G.R. and R.P.G., respectively).